

1 **Biogeochemical variations at the Porcupine Abyssal**
2 **Plain Sustained Observatory (PAP-SO) in the northeast**
3 **Atlantic Ocean, from weekly to inter-annual time scales**

4
5 S. E. Hartman^{1,*}, Z.-P. Jiang², D. Turk^{3,4}, R. S. Lampitt¹, H. Frigstad⁵,
6 C. Ostle^{6,7} and U.Schuster⁸

7
8 [1] {National Oceanography Centre, Southampton, SO14 3ZH, UK}

9 [2] {Ocean Collage, Zhejiang University, Hangzhou, 310012, China}

10 [3] {Dalhousie University, Halifax, B3H 4R2, Canada}

11 [4] {Lamont-Doherty Earth Observatory, Palisades, 10964, USA}

12 [5] {Norwegian Environment Agency, 0663, Oslo, Norway}

13 [6] {Sir Alister Hardy Foundation for Ocean Science, Plymouth, PL1 2PB, UK}

14 [7] {School of Environmental Sciences, University of East Anglia, Norwich, NR4 7TJ, UK}

15 [8] {University of Exeter, Exeter, EX4 4PS, UK}

16
17 Correspondence to: S.E.Hartman (suh@noc. ac.uk)

18
19 **Abstract**

20 We present high-resolution autonomous measurements of carbon dioxide partial pres-
21 sure $p(\text{CO}_2)$ taken *in situ* at the Porcupine Abyssal Plain sustained observatory (PAP- SO) in
22 the northeast Atlantic (49° N, 16.5° W; water depth of 4850 m) for the period 2010 to 2012.
23 Measurements of $p(\text{CO}_2)$ made at 30 m depth on a sensor frame are compared with other
24 autonomous biogeochemical measurements at that depth (including chlorophyll a-

1 fluorescence and nitrate concentration data) to analyse weekly to seasonal controls on $p(\text{CO}_2)$
2 flux in the inter-gyre region of the North Atlantic. Comparisons are also made with *in situ*
3 regional time-series data from a ship of opportunity and mixed layer depth (MLD)
4 measurements from profiling Argo floats. There is a persistent under saturation of CO_2 in
5 surface waters throughout the year which gives rise to a perennial CO_2 sink. Comparison with
6 an earlier dataset collected at the site (2003 to 2005) confirms seasonal and inter-annual
7 changes in surface seawater chemistry. There is year-to-year variability in the timing of deep
8 winter mixing and the intensity of the spring bloom.

9 The 2010–2012 period shows an overall increase in $p(\text{CO}_2)$ values when compared to
10 the 2003–2005 period as would be expected from increases due to anthropogenic CO_2
11 emissions. The surface temperature, wind speed and MLD measurements are similar for both
12 periods of time. Future work should incorporate daily CO_2 flux measurements made using
13 CO_2 sensors at 1 m depth and the *in situ* wind speed data now available from the UK Met
14 Office Buoy.

15

16 Keywords: carbon dioxide, nitrate, time-series, mooring buoys, ship of opportunity

17

18 Regional Index terms: North East Atlantic, Porcupine Abyssal Plain; geographic
19 bounding co-ordinates 48° N - 50° N, 16° W - 17° W

20

21 **1 Introduction**

22 A persistent feature of the subpolar North Atlantic is under-saturation of carbon
23 dioxide (CO_2) in surface waters throughout the year, which gives rise to a perennial CO_2 sink
24 (Körtzinger et al., 2008). This makes the north east Atlantic a region of great importance in
25 the global carbon cycle. There is evidence for inter-annual variation in the CO_2 sink ($1\text{--}3 \text{ mol}$
26 $\text{m}^{-2} \text{ a}^{-1}$) due to changes in wintertime mixing and stratification (Schuster and Watson, 2007).
27 Changes in the amount of CO_2 absorbed by the ocean may have implications for the global
28 carbon cycle now and for the role of the ocean as a carbon sink in the future. Studies of the
29 physical and biological processes regulating surface water $p(\text{CO}_2)$ (partial pressure of CO_2)

1 are required to estimate future trends in the ability of the ocean to act as a sink for increasing
2 CO₂ in the atmosphere. Frequent observations from fixed positions are critical to make these
3 calculations (McGillicuddy et al., 1998).

4 Accurate, high-resolution, long-term datasets are offered by time series studies such
5 as the Porcupine Abyssal Plain sustained Observatory (PAP-SO) in the northeast Atlantic at
6 49° N, 16.5° W (4850 m water depth) where a fixed-point mooring has been in place since
7 2002 (Hartman et al., 2012). The PAP-SO is in the North Atlantic Drift Region, a
8 biogeographical province defined by deep winter convective mixing (Longhurst, 2006;
9 Monterey and Levitus, 1997). The surface mixed layer depth can change from 25 m in the
10 summer to over 400 m in winter. A twofold decrease in winter nitrate concentration over a
11 three year period from 2003 has been attributed to a combination of shallower winter
12 convective mixing and changes in surface circulation (Hartman et al., 2010). The PAP-SO is
13 in an area with relatively high wind speeds, frequently greater than 10 m s⁻¹. High wind
14 speeds have a significant effect on CO₂ flux (Takahashi et al., 2002). The CO₂ flux at the
15 PAP-SO was calculated from $p(\text{CO}_2)$, between 2003 and 2005 as a net flux into the ocean of
16 over 3 mol m⁻² a⁻¹ (Körtzinger et al., 2008). This is a significant sink compared with
17 subtropical time series sites such as ESTOC (near the Canary Islands, 29.17° N, 15.5° W),
18 which is an overall annual CO₂ source region (0.05 mol m⁻² a⁻¹, Gonzalez-Davila et al.,
19 2003).

20 Recently, the decline in North Atlantic CO₂ uptake from 1994/1995 to 2002–2005 has
21 been linked to a variation in the North Atlantic Oscillation (Schuster and Watson, 2008;
22 Padin et al., 2011). The decreased uptake may be a consequence of declining rates of
23 wintertime mixing and ventilation between surface and subsurface waters due to increasing
24 stratification. Enhanced stratification forms a barrier to nutrient exchange, which may result
25 in a progressive decline in primary production (Field et al., 1998), as was seen in the North
26 Atlantic between 1999 and 2004 (Behrenfeld et al., 2006). The observed decrease in nitrate
27 concentration and productivity in this region (Behrenfeld et al., 2006), may in turn affect the
28 oceanic uptake of $p(\text{CO}_2)$.

29 In this paper, we present recent year round time-series data of temperature, salinity,
30 nitrate concentration, chlorophyll a-fluorescence and $p(\text{CO}_2)$ collected at 30 m depth from
31 May 2010 to June 2012. The data are compared with an earlier published dataset (from July
32 2003 to July 2005) and additional $p(\text{CO}_2)$ measurements made from a ship of opportunity.

1 The *in situ* dataset is considered in relation to convective mixing processes using mixed layer
2 depth (MLD) estimates calculated from profiling Argo floats. The weekly air-sea CO₂ flux at
3 the PAP-SO site was calculated from *in situ* $p(\text{CO}_2)$ measurements and ancillary satellite
4 wind speed datasets. The objective of this study is to examine the biogeochemical variations
5 at the PAP-SO in the northeast Atlantic over different periods from weekly, seasonal to
6 annual.

7

8 **2 Materials and methods**

9 **2.1 Study site**

10 The position of the Porcupine Abyssal Plain sustained observatory (PAP-SO) at 49°
11 N, 16.5° W is shown in Fig. 1. Lampitt et al. (2001) has summarised the hydrography,
12 meteorology and upper mixed layer dynamics in the region.

13

14 **2.2 In Situ data**

15 The instrumentation of the PAP-SO observatory has been described in detail by
16 Hartman et al., 2012 (see Table 1 and Fig. 1 therein) and is briefly summarized here. Since
17 2002 instruments on a mooring at the PAP-SO (49° N, 16.5° W) have recorded a suite of
18 parameters in the mixed layer. Temperature and salinity measurements were made on a frame at a
19 nominal depth of 30 m, using Seabird SBE 37-IM MicroCAT recorders (Sea-Bird Electronics Inc.,
20 Bellevue, Washington, USA). Measurements of nitrate concentration, chlorophyll a-
21 fluorescence and $p(\text{CO}_2)$, were also made using biogeochemical sensors on the frame, often
22 within the deep chlorophyll maximum. Between 2002 and 2007 the sensor frame depth varied
23 from 20 m to 225 m, deflecting in response to local currents. A surface buoy was added in
24 2007 so that measurements were consistently made at 30 m depth. In 2010 collaboration with
25 the UK Met Office led to a redesigned infrastructure, providing simultaneous surface
26 physical and biogeochemical measurements with surface meteorological data.

27 $p(\text{CO}_2)$ data during the two periods of time examined here were collected using
28 different instrumentation. From 2003–2005 it was measured using a SAMI (Sunburst Sensors
29 LLC, USA) sensor, which is based on equilibration of a pH indicator solution, contained in a

1 gas-permeable membrane, with ambient $p(\text{CO}_2)$ and subsequent spectrophotometric
2 determination in the equilibrated solution (DeGrandpre et al., 1995). Twice daily $p(\text{CO}_2)$
3 measurements, from 2010 to 2012, were made using a membrane-based PRO-CO2 sensor
4 (Pro-Oceanus, Canada), which uses an infrared detector and is internally calibrated through
5 an auto-zero calibration function (Jiang et al., 2014). Note that a measurement error of an
6 early version of the PRO-CO2 sensor during the deployment, induced by the fluctuation of
7 detector cell temperature, was identified and corrected (see Jiang et al., 2014 for further
8 details). A pump was used (Seabird Inc.) to improve water flow across the sensor membrane
9 to accelerate attaining equilibrium. The surface *in situ* $p(\text{CO}_2)$ time-series ceased between
10 2006 and 2009 due to funding issues.

11 Although measured by different instruments, the two $p(\text{CO}_2)$ data sets were calibrated
12 in a similar way to make them comparable: the sensor outputs were calibrated against $p(\text{CO}_2)$
13 values calculated from dissolved inorganic carbon (DIC) and total alkalinity (TA) from
14 discrete samples taken at the mooring site during deployment/recovery cruises; and
15 plausibility checks were made with underway $p(\text{CO}_2)$ measurements around the PAP site.
16 The 2003-2005 data were previously published (see Körtzinger et al., 2008 for details) with a
17 precision of 1 μatm and accuracy estimated as 6-10 μatm . The 2010-2012 data have a similar
18 precision (1 μatm) and accuracy (6 μatm).

19 A Hobi Labs Inc., HS-2 fluorometer (Arizona, USA) was used on the PAP-SO
20 mooring to estimate chlorophyll a concentration until 2005 when an alternative ECO FLNTU
21 (WETlab, USA) fluorometer came into use. The quoted precision for fluorescence measured
22 by these fluorometers is 0.04%, however as described by Hartman et al., (2010), fluorescence
23 output can only provide an approximation of the chlorophyll a concentration. The
24 fluorescence/chlorophyll a concentration ratio changes throughout the year, due to variations
25 in the phytoplankton species composition. On the mooring, chlorophyll a-fluorescence
26 measurements were taken every 2 hours over the 1 year deployments and biofouling was
27 controlled using motorised copper shutters on each of the fluorometers.

28 Nitrate concentration measurements were initially made using wet chemical NAS
29 Nitrate Analysers (EnviroTech LLC, USA), precision 0.2 $\mu\text{mol l}^{-1}$, as described in Hydes et
30 al. (2000), with twice daily sampling frequency and internal calibration as described by
31 Hartman et al. (2010). From 2010 additional higher frequency inorganic nitrate

1 measurements were made using UV detection methods (ISUS, Satlantic), with a precision of
2 $1 \mu\text{mol l}^{-1}$.

3 For each instrument the manufacturer's calibration was checked at the start of each
4 deployment and a correction for instrument drift was made using a second calibration check
5 on recovery of the instruments. Biogeochemical data from the PAP-SO are available from
6 www.eurosites.info/pap and the British Oceanographic Data Centre (BODC). Data presented
7 here cover the period when $p(\text{CO}_2)$ measurements are available, July 2003 to the end of June
8 2005 (with deployments in July 2003, November 2003, June 2004) and the period from May
9 2010 to June 2012 (with sensor deployment in May 2010, September 2010, July 2011, May
10 2012). All of the measurements are within the mixed layer although the depth of
11 measurements is closer to the 30 m nominal depth after mooring redesign to incorporate a
12 surface float in 2007.

13

14 **2.3 Other observational data sources**

15 Temperature and salinity data were taken from Argo floats
16 (<http://www.coriolis.eu.org>), extracting (30 ± 5) m depth data. To obtain a continuous
17 seasonal description, a large region around the PAP site was selected (45°N to 52°N and
18 26.08°W to 8.92°W , excluding the shelf area). The Argo data have a potentially lower
19 accuracy (0.005°C for temperature and 0.1 for salinity) than the *in situ* MicroCAT data
20 (0.002 for salinity and 0.002°C for temperature). However the Argo data were chosen over
21 the *in situ* data for all calculations as they have a larger temporal coverage and are internally
22 consistent.

23 The $p(\text{CO}_2)$ time-series was compared with surface data from a ship of opportunity
24 (SOO) running from Portsmouth, UK to the Caribbean (Schuster et al., 2007). Onboard the
25 SOO continuous $p(\text{CO}_2)$ measurements are made using a calibrated system with a
26 showerhead equilibrator (Schuster et al., 2007). Data are available from the Surface ocean
27 CO_2 atlas (SOCAT) <http://www.socat.info/>. Discrete nutrient samples were collected at 4
28 hour intervals along the same route and were analysed ashore (Hartman et al., 2008). This
29 provides an approximately monthly nutrient sample and $p(\text{CO}_2)$ data points close to the PAP-
30 SO on the return route of the ship. The nominal depth of these samples is 5 m, which is
31 shallower than the 30 m samples from the PAP-SO. We selected SOO data between 52°N

1 and 45° N and 8.92° W and 26.08° W, and then took the average $p(\text{CO}_2)$ values that were
2 within that area on the same day as the sample from the PAP-SO site.

3 Through collaboration with the UK Met Office *in situ* wind speed data are available
4 since 2010. However for consistency in calculations of CO_2 flux between the two time
5 periods (2003–2005 and 2010–2012) considered here we took wind speed data from weekly
6 satellite data: Fleet Numerical Meteorology and Oceanography Center (FNMOC) 1° by 1°.
7 We calculated a weekly mean from the 6 hourly, 10 m height data; available from
8 <http://las.pfeg.noaa.gov/>.

9 The air-sea CO_2 flux (in $\text{mmol m}^{-2} \text{d}^{-1}$) was calculated from the air-sea $p(\text{CO}_2)$
10 difference, temperature and salinity (30 m) and wind speed at 10 m height, using the
11 following equation:

$$12 \quad F(\text{CO}_2) = k \cdot K_0 [p(\text{CO}_{2\text{sea}}) - p(\text{CO}_{2\text{air}})] \quad (1)$$

13 Where k is the transfer coefficient based on the wind speed-dependent formulation of
14 Nightingale et al. (2000), scaled to the temperature-dependent Schmidt number according to
15 Wanninkhof (1992), K_0 is the CO_2 solubility at the *in situ* temperature and salinity after
16 Weiss (1974). While $p(\text{CO}_2, \text{sea})$ and $p(\text{CO}_2, \text{air})$ are the CO_2 partial pressures of seawater
17 and average CO_2 dry mole fraction measured in air, respectively. As $p(\text{CO}_2)$ was reported
18 throughout this manuscript, we used $p(\text{CO}_2)$ for the air-sea flux calculation. Using $f(\text{CO}_2)$ for
19 the calculation would generate the same results of flux estimates. The atmospheric $p(\text{CO}_2)$ is
20 calculated from monthly averaged $x(\text{CO}_2)$ measured at Mace Head (53.33° N, 9.90° W)
21 assuming 100 % water vapour saturation under 1 atm air pressure. Please note that 1 atm =
22 1.01325 bar. This is an appropriate pressure to use at the PAP-SO as the average (and
23 standard deviation) of the air pressure, measured on the buoy at the PAP-SO between
24 September 2010 to July 2011, was (1.01354 ± 13.14) bar.

25 Total alkalinity (TA) was calculated from Argo temperature and salinity (30 m),
26 following the relationship for the North Atlantic developed by Lee et al. (2006) with an
27 uncertainty of $\pm 6.4 \mu\text{mol kg}^{-1}$ (Lee et al., 2006). The DIC concentration was then calculated
28 from TA and $p(\text{CO}_2)$ using the “seacarb” package (Lavigne and Gattuso, 2011), with Argo
29 temperature and salinity (30 m) and nutrient concentrations set to zero. The chosen constants
30 were Lueker et al. (2000) for K_1 and K_2 , Perez and Fraga (1987) for K_f and the Dickson

1 (1990) constant for K_s , as recommended by Dickson et al. (2007). We followed Körtzinger et
2 al. (2008)'s method to correct the DIC changes driven by air-sea exchange:

$$3 \quad \Delta \text{DIC}_{\text{gas}} = F(\text{CO}_2) / \text{MLD}.$$

4 Using TA and $p(\text{CO}_2)$ to calculate DIC, and taking the various uncertainties in the
5 calculation into account, introduces an error in the order of $7.0 \mu\text{mol kg}^{-1}$.

6 The MLD was calculated from density profiles using global gridded fields of
7 temperature and salinity collected by Argo floats, XBTs, CTDs and moorings. These data are
8 collected and made freely available by the Coriolis project and programmes that contribute to
9 it (<http://www.coriolis.eu.org>). We used the near real time mode data as these datasets have
10 been quality control checked. Before deciding on a MLD definition an inter-comparison of
11 many definitions commonly used in the literature was done such as density differences,
12 temperature differences and density gradients (Kara et al. 2000; Thomson and Fine 2003;
13 Montegut et al. 2004). A subset of the global density profiles calculated from the gridded
14 temperature and salinity fields was used to compare the different methods. The depth of the
15 mixed layer was estimated through visual inspection of over 3000 profiles, following a
16 similar approach used by Fiedler (2010). The Holte and Talley (2009) density difference
17 algorithm gave the closest match with the visually estimated MLD (RMSD 29.38 m). The
18 depth of the mixed layer was defined by a density difference of 0.03 kg m^{-3} from the density
19 at a reference depth (in this case 10 m to avoid diurnal changes in temperature and salinity at
20 the surface). This Holte and Talley (2009) density difference algorithm incorporates linear
21 interpolation to estimate the depth at which the density difference is crossed.

22 The North Atlantic Oscillation (NAO) index (after Hurrell, 1995) was obtained from
23 the University of East Anglia web site <http://www.cru.uea.ac.uk/cru/data/nao/>.

24

25 **3 Results**

26 Figures 2a–c show the *in situ* observations from the PAP-SO at 30 m depth, including
27 $p(\text{CO}_2)$, chlorophyll a-fluorescence and nitrate concentration. Figure 2a shows the range of
28 $p(\text{CO}_2)$ from 2003 to 2005, which was also shown in Körtzinger et al. (2008). The range was
29 $74 \mu\text{atm}$ (300 to $374 \mu\text{atm}$) and the mean was $339 \mu\text{atm}$. In comparison, $p(\text{CO}_2)$ between
30 2010 and 2012 had a $57 \mu\text{atm}$ range (327 to $384 \mu\text{atm}$) with a higher mean of $353 \mu\text{atm}$. The

1 $p(\text{CO}_2)$ data for the 2010–2012 period are confirmed by SOO data from the Portsmouth to
2 Caribbean route in Fig. 2a (see Fig. 1 for positions of the SOO samples). Körtzinger et al.
3 (2008) also reported a good comparison with a SOO route from Kiel, to the north of the
4 Portsmouth to Caribbean route, for the 2003–2005 data. The SOO data fill in the gap in the
5 time series when PAP-SO $p(\text{CO}_2)$ data were not available due to failure of the instrument
6 logger. The higher $p(\text{CO}_2)$ values in the 2010 to 2012 period are confirmed by the SOO data.

7 *In situ* chlorophyll data in Fig. 2b shows the characteristic chlorophyll a-fluorescence
8 increase for this area during the spring bloom. There is large inter-annual variability in both
9 the timing and magnitude of the spring bloom for the two time periods shown. For example
10 the spring bloom in 2004 started in late May compared with an earlier bloom in 2011 (that
11 started in April). The increase in chlorophyll a fluorescence during the 2011 spring bloom
12 was also larger compared with the other years shown.

13 Nitrate concentration data in Fig. 2c shows the characteristic seasonality, with
14 increased winter nitrate concentrations and depletion following the spring bloom (seen in Fig.
15 2b). The seasonality in the nitrate concentration is similar for the two periods shown (2003–
16 2005 and 2010–2012). SOO nitrate concentration data show a good agreement with the PAP-
17 SO data throughout 2010–2012 and fill in the gaps in early 2011 when nutrient measurements
18 at the PAP-SO are not available. Overall, the *in situ* data show a characteristic increase in
19 inorganic nitrate concentrations, and $p(\text{CO}_2)$, through the winter as fluorescence decreases.
20 However, winter nitrate concentrations are significantly lower in the 2004/2005 winter
21 compared with other years as has been discussed in Hartman et al., (2010).

22 Fig. 3a shows the Argo temperature data extracted at 30 m depth and the *in situ*
23 MicroCAT temperature data at the PAP-SO. Temperature shows opposite seasonal variations
24 to the $p(\text{CO}_2)$ and nitrate concentration from *in situ* data. A comparison of Argo temperature
25 with *in situ* 30 m MicroCAT data (n=112, comparison not shown) suggests errors of up to 1
26 % for temperature in the Argo data compared with the *in situ* data (when available). Both
27 datasets show that the temperature variations in these years are very similar, showing a
28 summer-winter difference of 6 °C (Fig.3a).

29 The seasonality of the *in situ* data can be put in context when looking at the MLD in
30 Fig. 3b. The increase in $p(\text{CO}_2)$ and nitrate concentration corresponds to deeper convective
31 mixing in winter. The MLD range varies little over the winters considered here (Fig. 3b) and

1 the maximum MLD does not exceed 260 m. However the timing of the maximum winter
2 mixed layer depth at PAP-SO varies from year to year. For example the maximum MLD
3 (Fig. 3b) for the 2010/2011 winter reached 215 m in February 2011 compared with earlier
4 and deeper mixing (to 257 m) in the following 2011/2012 winter (December 2011).

5 The calculated DIC concentrations (Fig. 3c) show a closer relationship to the MLD
6 seasonality than nitrate concentration data. Seasonal variation in the concentration of both
7 DIC and nitrate is similar apart from the 2004/2005 winter; when low DIC concentrations
8 were not seen at the same time as the low nitrate concentrations (Fig.3c).

9 The interrelation between DIC and nitrate concentrations can be considered by
10 comparing the C : N ratios to the Redfield ratio (Redfield, 1958). The 2003-2005 time period
11 has already been considered in Körtzinger et al. (2008) so is not reproduced here. Following
12 Körtzinger et al. (2008) we calculated DIC, corrected for gas exchange. DIC concentrations
13 were plotted against the *in situ* nitrate concentrations in different seasons for 2010-2012 (Fig.
14 4). The C: N ratio differed from the Redfield ratio of 6.6 with especially high values in spring
15 (14.3).

16 Figure 5a shows weekly satellite wind speed data used to calculate the CO₂ flux. The
17 wind speeds were similar in the two periods. There is an earlier period of days with high wind
18 speeds towards the end of 2011 that can be compared with the CO₂ data presented. The
19 annual average wind speed was 8.2 m s⁻¹ for both time periods. The maximum was 14 m s⁻¹,
20 although *in situ* winds of up to 20 m s⁻¹ were seen from the Met Office data
21 (eurosites.info/pap), this is not seen in the weekly averaged satellite wind speed data
22 presented.

23 Figure 5b shows the sea-to-air CO₂ flux (where a positive flux is defined as from sea
24 to the atmosphere). This was calculated from *in situ* $p(\text{CO}_2)$ data and satellite wind speed data
25 (Fig. 5b). The week by week variation in CO₂ flux is shown and an overall average for the
26 two periods of time has been calculated as (-5.7 ± 2.8) mmol m⁻² d⁻¹ for the 2003–2005
27 period and (-5.0 ± 2.2) mmol m⁻² d⁻¹ for the 2010–2012 period. SOO data have been used at
28 the start of 2011 when *in situ* $p(\text{CO}_2)$ data were unavailable. The start and end months of the
29 two periods of time differs, which will contribute to the errors in the flux measurements.
30 However the errors are comparable for the two periods of time considered and overall the
31 average for the two time periods is similar.

1 There is little variation in CO₂ flux and MLD between the years shown but for
2 completeness the NAO index is shown in Fig. 5c. The 2003/2004 winter NAO was near zero
3 and the 2004/2005 winter NAO was also low, between -2 to +1. In contrast there is a large
4 range in the winter NAO in the 2010/2011 winter when the NAO changed from -4 to +3.
5 Overall the range in the NAO values was larger for the 2010 to 2012 time period shown.

7 **4 Discussion**

8 **4.1 PAP-SO seasonal variation**

9 The 2003–2005 and 2010–2013 datasets show very similar seasonal patterns between
10 the years. Concentrations of nitrate and DIC exhibit seasonal variations opposite to
11 temperature. The seasonal variation in nitrate and DIC concentrations is controlled by
12 convective mixing (resulting in the winter maximum) and biological uptake during the spring
13 bloom period (resulting in the summer minimum), which is similar to elsewhere in the North
14 Atlantic (Jiang et al. 2013).

15 The $p(\text{CO}_2)$ distribution pattern at the PAP-SO site is characterized by a single annual
16 peak (high in winter and low in summer), which is similar to that of nutrient and DIC
17 concentrations, but in antiphase to the temperature signal. Jiang et al. (2013) compared
18 seasonal carbon variability between different sites in the North Atlantic and suggested a
19 latitudinal change in $p(\text{CO}_2)$ seasonality from the temperature-dominated oligotrophic
20 subtropical gyre to the subpolar region where $p(\text{CO}_2)$ is dominated by changing
21 concentrations of DIC. Our $p(\text{CO}_2)$ observations at the PAP-SO site show the subpolar-like
22 seasonal pattern, which is similar to that of the Ocean Weather Station M (Skjelvan et al.,
23 2008). The surface $p(\text{CO}_2)$ is mainly governed by the varying DIC concentration while the
24 seasonal cooling and warming have a contrasting effect.

25 The time integrated uptake of DIC and nitrate during the spring bloom is reflected by
26 the slope of the linear regression between them (Fig. 4). The ratio of DIC and nitrate
27 concentrations from 2010-2012 shows higher values than the Redfield C : N ratio of 6.6. For
28 example the spring-time ratio of 14.3 (± 5) was considerably higher than the Redfield ratio, in
29 agreement with similar “carbon overconsumption” ratios seen for the North Atlantic (e.g.
30 14.2, Sambrotto et al., 1993). This value is in agreement with the single C : N ratio reported

1 previously at the PAP-SO of 11.0 (Körtzinger et al., 2008). In both cases the DIC
2 concentrations were calculated and therefore associated with errors in the order of 7.0 μmol
3 kg^{-1} . We have demonstrated seasonal variation in the C : N ratio at the PAP-SO, with an
4 autumn C : N value that is closer to the Redfield ratio and large deviations from the Redfield
5 ratio in winter.

7 **4.2 Air-sea CO₂ flux**

8 Wind speeds have an indirect impact on the biogeochemistry, in particular $p(\text{CO}_2)$. In
9 the North Atlantic the strength and frequency of wintertime storms is significantly increasing
10 (Donat et al., 2011). Wind speeds are similar for the two time periods considered here.
11 However there is some suggestion of an earlier increase in winds at the start of the 2011/2012
12 winter (Fig. 5a) coinciding with an earlier increase in mixing (Fig. 3b). Although the CO₂
13 flux is not linked linearly to the wind speed there is a corresponding decrease in CO₂ flux into
14 the ocean at this time.

15 It is well known that the northeast Atlantic is a strong CO₂ sink with large variability.
16 The observations at the PAP-SO provide high frequency data to follow the variability in CO₂
17 exchange. The largest CO₂ flux shown here was in September 2004, as a combined result of
18 low seawater $p(\text{CO}_2)$ (Fig. 2a) and high wind speed (Fig. 5b). Larger CO₂ flux into the ocean
19 may have occurred in 2011 considering the large, early spring bloom seen in that year but we
20 do not have *in situ* PAP-SO $p(\text{CO}_2)$ data to calculate the flux at that time. However flux
21 calculations from SOO data in early 2011 do not suggest an increase in CO₂ flux. Increases in
22 productivity do not necessarily result in enhanced oceanic CO₂ uptake as the gas exchange is
23 also affected by other factors such as temperature and wind speed (Dumousseaud et al., 2010;
24 Jiang et al., 2013). The average is similar for the years presented with values of -5.7 mmol
25 $\text{m}^{-2} \text{d}^{-1}$ in 2003–2005 and -5.0 $\text{mmol} \text{m}^{-2} \text{d}^{-1}$ from 2010–2012.

27 **4.3 PAP-SO inter-annual variations**

28 It is suggested that NAO plays an important role in modulating the inter-annual
29 variability in the northeast Atlantic region by affecting the intensity of winter convection
30 (Bennington et al., 2009; Jiang et al., 2013). The Gibraltar minus Iceland version of the NAO

1 index is really most applicable to the winter half of the year. During positive NAO periods,
2 the PAP-SO region experiences subpolar-like conditions, with strong wind stress and deep
3 mixed layers (Henson et al., 2012). However the MLD did not vary significantly at the PAP-
4 SO between the 2003–2005 and 2010–2012 time periods shown here (with a range of only
5 215 to 257 m for deepest winter MLD between the years. In previous years such as
6 2009/2010 deep winter mixing of 390 m has been seen with an NAO reaching -3, (not
7 shown). NAO is unlikely to have a large role as the PAP-SO as winter sea surface
8 temperature and MLD were similar in the time periods from 2003–2005 and 2010–2012.
9 Data from a winter with deeper mixing would need to be put into the comparison to resolve
10 this.

11 There was a twofold decrease in nitrate concentrations in the 2004/05 winter despite
12 sea surface temperature and MLD values being close to other years. The low values were
13 confirmed by SOO data, also shown in Hartman et al. (2010). As discussed in Hartman et al.
14 (2010) the lower winter nitrate concentration seen in 2004/2005 did not correlate with a
15 decrease in the MLD and this showed the influence of horizontal mixing at the PAP-SO. It
16 was suggested that lateral advection to the site at that time introduced a subtropical water
17 mass with a lower nitrate concentration. Earlier time-series studies largely ignored circulation
18 at the PAP-SO site, assuming convective mixing is a dominant process influencing mixed
19 layer temperature and nitrate concentrations in the region (Williams et al., 2000; Körtzinger
20 et al. 2008). However, fixed-point time-series observations are influenced by spatial
21 variability passing the point of observation (McGillicuddy et al., 1998; Painter et al., 2010). It
22 is clear from Hartman et al. (2010) that lateral advection may significantly influence the
23 surface temperature and nitrate concentrations in the region of the PAP-SO site.

24 The observed seawater $p(\text{CO}_2)$ increased from $(339 \pm 17) \mu\text{atm}$ in 2003-2005 to $(353$
25 $\pm 15) \mu\text{atm}$ in 2010-2012, which largely agrees with the increasing rate of surface seawater
26 $p(\text{CO}_2)$ observed in the North Atlantic basin of $(1.84 \pm 0.4) \mu\text{atm a}^{-1}$ (Takahashi et al. 2009).
27 Despite similar maximum winter MLD in 2003–2005 and 2010–2012, the timing and
28 intensity of the spring bloom is quite different and the cause of this requires further
29 investigation.

30

31 **5 Conclusions and further work**

1 We have presented recent year round surface time-series biogeochemical data at the
2 PAP-SO and compared it with previous observations. The surface $p(\text{CO}_2)$, and concentrations
3 of DIC and nitrate, at the PAP-SO all show a clear seasonal cycle, which is mainly controlled
4 by winter convective mixing and biological activity in the spring bloom. However the
5 suggestion that inter-annual variability is dominated by convection (Bennington et al., 2009)
6 is not clear as the MLD did not vary significantly between the winter periods shown. An
7 especially low winter nitrate concentration in 2005 was observed, thought to be due to
8 surface advection and this highlights the need to consider advection when dealing with time
9 series data in the future. Despite the similar winter physical conditions (temperature and
10 MLD), there is a year to year difference in the timing and intensity of the spring blooms,
11 which requires further investigation. At PAP-SO, increasing mean seawater $p(\text{CO}_2)$ from
12 $(339 \pm 17) \mu\text{atm}$ in 2003 to $(353 \pm 15) \mu\text{atm}$ in 2011 was observed. However the mean air-sea
13 CO_2 flux did not show a significant change. It varied from $(-5.7 \pm 2.8) \text{mmol m}^{-2} \text{d}^{-1}$ in 2003-
14 2005 to $(-5.0 \pm 2.2) \text{mmol m}^{-2} \text{d}^{-1}$ in 2010-2012.

15 In 2010, collaboration between the UK's Natural Environment Research Council
16 (NERC) and Meteorological Office led to the first simultaneous monitoring of *in situ*
17 meteorological and ocean variables at the PAP-SO (Hartman et al., 2012). From 2013
18 additional measurements of $p(\text{CO}_2)$ will be made at the site, at the shallower depth of 1 m,
19 and should further improve the SOO comparison. The site could be used to investigate the
20 effect of different parameterizations (Prytherch et al., 2010) and wind products on
21 calculations of CO_2 flux, in particular during the high wind conditions seen. Using the
22 contemporaneous atmospheric and ocean datasets we will be able to investigate the effect of
23 storms on CO_2 flux and resolve daily variability.

24

25 **Acknowledgements**

26 We would like to acknowledge the various ship crew, engineers and scientists involved in
27 preparation, deployment and recovery of the PAP-SO moorings. We would especially
28 like to thank J. Campbell, M. Hartman and M. Pagnani for the PAP time series and H. Cole
29 who calculated MLD from the Argo float data. The research leading to these results was
30 supported through the EU FP7 project CARBOCHANGE “Changes in carbon uptake and
31 emissions by oceans in a changing climate”, which received funding from the European

1 Commission's Seventh Framework Programme under grant agreement no. 264879. Funding
2 that supports the running of the SOO network used in this project also includes EU grant
3 212196 (CO- COS), and UK NERC grant NE/H017046/1 (UKOARP); Funding for part of
4 this study was provided by NERC CASE studentship grant reference number NE/J500069/1
5 in collaboration with SAHFOS. Argo data were made freely available by the Coriolis project
6 and programmes that contribute to it <http://www.coriolis.eu.org>. FNMOC wind speed data
7 were available from <http://las.pfeg.noaa.gov>. Mooring data and support for this research was
8 provided by the European research projects ANIMATE (Atlantic Network of
9 Interdisciplinary Moorings and Time- Series for Europe), MERSEA (Marine Environment
10 and Security for the European Sea), EUR- OCEANS (European Network of Excellence for
11 Ocean Ecosystems Analysis) and EuroSITES grant agreement EU 202955. The work was
12 also supported through the Natural Environment Research Council (NERC), UK, project
13 Oceans 2025 and National Capability. The PAP-SO also contributes to the EU funded FixO3
14 project EU 312463 and the NERC Greenhouse Gas TAP NE/k00249x/1. D. Turk was
15 supported by the Canada Excellence Research Chair (CERC) in Oceans Science and
16 Technology. LDEO contribution number 7768.

17

18 **References**

19

20 Behrenfeld, M. J., O'Malley, R. T., Siegel, D. A., McClain, C. R., Sarmiento, J. L., Feldman,
21 G. C., and Milligan, A. J.: Climate-driven trends in contemporary ocean productivity, *Nature*,
22 444, 752–755, 2006.

23 Bennington, V., McKinley, G. A., Dutkiewicz, S., and Ullman, D.: What does chlorophyll
24 variability tell us about export and air-sea CO₂ flux variability in the North Atlantic?, *Global*
25 *Biogeochem. Cy.*, 23, GB3002, doi:10.1029/2008GB003241., 2009.

26 DeGrandpre, M. D., Hammar, T. R., Smith, S. P., and Sayles, F. L.: In situ measurements of
27 seawater pCO₂, *Limnol. Oceanogr.*, 40, 969–975, 1995.

28 Dickson, A. G.: Standard potential of the (AgCl(s) + 1/2H₂(g)=Ag(s) + HCl(aq)) cell and
29 the dissociation constant of bisulfate ion in synthetic sea water from 273.15 to 318.15 K, *J.*
30 *Chem. Thermodyn.*, 22, 113–127, doi:10.1016/0021-9614(90)90074-Z, 1990.

- 1 Dickson, A. G., Sabine, C. L., and Christian, J. R.: Guide to Best Practices for Ocean CO₂
2 Measurements, PICES Special Publication 3, Sidney, British Columbia. 191 pp., 2007.
- 3 Donat, M. G., Renggli, D., Wild, S., Alexander, L. V., Leckebusch, G. C., and Ulbrich,
4 U.: Reanalysis suggests long-term upward trends in European storminess since 1871.
5 *Geophys. Res. Lett.*, 38, L14703, 2011.
- 6 Fiedler, P.C.: Comparison of objective descriptions of the thermocline. *Limnology and*
7 *Oceanography-Methods*, 8, 313-325, 2010.
- 8 Field, C. B., Behrenfeld, M. J., and Randerson, J. T.: Primary production of the biosphere:
9 integrating terrestrial and oceanic components, *Science*, 281, 237–240, 1998.
- 10 González-Dávila, M., Santana-Casiano, J. M., Rueda, M. J., Llinas, O., and Gonzalez-
11 Davila, E. F.: Seasonal and interannual variability of sea-surface carbon dioxide species at the
12 European Station for Time Series in the Ocean at the Canary Islands (ESTOC) between 1996
13 and 2000., *Global Biogeochem. Cy.*, 17, 1076, doi:10.1029/2002gb001993, 2003.
- 14 Hartman, S. E., Larkin, K. E., Lampitt, R. S., Lankhorst, M., and Hydes, D. J.: Seasonal and
15 inter-annual biogeochemical variations in the Porcupine Abyssal Plain 2003–2005 associated
16 with winter mixing and surface circulation, *Deep-Sea Res. II*, 57, 1303–1312, 2010.
- 17 Hartman, S. E., Lampitt, R. S., Larkin, K. E., Pagnani, M., Campbell, J., Gkritzalis, A., and
18 Jiang, Z. P.: The Porcupine Abyssal Plain fixed-point sustained observatory (PAP-SO):
19 variations and trends from the Northeast Atlantic fixed-point time-series, *ICES J. Mar. Sci.*,
20 57, 776–783, 2012.
- 21 Henson, S., Lampitt, R., and Johns, D.: Variability in phytoplankton community structure in
22 response to the North Atlantic Oscillation and implications for organic carbon flux, *Limnol.*
23 *Oceanogr.*, 57, 1591, 2012.
- 24 Holte, J. and Talley, L.: A New Algorithm for Finding Mixed Layer Depths with
25 Applications to Argo Data and Subantarctic Mode Water Formation, *J. Atmos. Ocean. Tech.*,
26 26, 1920–1939, 2009.
- 27 Hurrell, J. W.: Decadal trends in the North Atlantic oscillation: regional temperatures and
28 precipitation, *Science*, 269, 676–679, 1995.

1 Hydes, D. J., Wright, P. N., and Rawlinson, M. B.: Use of a wet chemical analyser for the *in*
2 *situ* monitoring of nitrate, Chemical sensors in Oceanography, in: Chemical Sensors in
3 Oceanography, edited by: Varney, M., Gordon and Breach, Amsterdam, 95–105, 2000.

4 Jiang, Z-P, Hydes, D.J, Tyrrell, T., Hartman, S. E., Hartman, M. C., Dumousseaud, C., Padin,
5 X. A., Skjelvan, I., and González-Pola, C.: Key controls on the seasonal and inter- annual
6 variations of the carbonate system and air-sea CO₂ flux in the Northeast Atlantic (Bay of
7 Biscay), J. Geophys. Res.-Oceans, 118, 785–800, 2013.

8 Jiang, Z-P, Hydes, D.J, Tyrrell, T., Hartman, S. E., Hartman, M. C., Campbell, J. M.,
9 Johnson, B. D., Schofield, B., Turk, D., Wallace, D, Burt, W., Thomas, H., Cosca, C., and
10 Feely, R.: Application and assessment of a membrane-based pCO₂ sensor under field and
11 laboratory conditions, Limnol. Oceanogr.-Meth., 12, 264–280, 2014.

12 Kara, A.B., Rochford P.A. and Hurlburt H.E.: An optimal definition for ocean mixed layer
13 depth. Journal of Geophysical Research-Oceans, 105(C7), 16803-16821, 2000.

14 Körtzinger, A., Send, U., Lampitt, R.S., Hartman, S., Wallace, D. W. R., Karstensen, J.,
15 Villagarcia, M. G., Llinás, O., and DeGrandpre, M. D.: The seasonal pCO₂ cycle at 49°
16 N/16.5° W in the northeastern Atlantic Ocean and what it tells us about biological
17 productivity, J. Geophys. Res., 113, C04020, doi:10.1029/2007jc004347, 2008.

18 Lampitt, R. S., Bett, B. J., Kiriakoulis, K., Popova, E., Ragueneau, O., Vangriesheim, A., and
19 Wolff, G. A.: Material supply to the abyssal seafloor in the Northeast Atlantic, Prog.
20 Oceanogr., 50, 27–63, 2001.

21 Lavigne, H. and Gattuso, J.-P.: Seacarb: seawater carbonate chemistry with R. R package
22 version 2.4., <http://CRAN.R-project.org/package=seacarb>., edited., 2011.

23 Lee, K., Tong, L. T., Millero, F. J., Sabine, C. L., Dickson, A. G., Goyet, C., Park, G. H.,
24 Wanninkhof, R., Feely, R. A., and Key, R. M.: Global relationships of total alkalinity with
25 salinity and temperature in surface waters of the world's oceans, Geophys. Res. Lett., 33,
26 L19605,doi:10.1029/2006gl027207, 2006.

27 Longhurst, A.: Ecological geography of the sea, Ecological Geography of the Sea Series, 2nd
28 ed., 560 pp., Academic Press, San Diego, 2006.

1 Lueker, T. J., Dickson, A. G. and Keeling, C. D.: Ocean pCO₂ calculated from dissolved in-
2 organic carbon, alkalinity, and equations for K-1 and K-2: validation based on laboratory
3 measurements of CO₂ in gas and seawater at equilibrium, *Mar. Chem.*, 70, 105–119, 2000.

4 McGillicuddy, D. J., Robinson, A. R., Siegel, D. A., Jannasch, H. W., Johnson, R., Dickey,
5 T. D., McNeil, J., Michaels, A. F., and Knap, A. H.: Influence of mesoscale eddies on new
6 production in the Sargasso Sea, *Nature*, 394, 263–266, 1998.

7 McKinley, G. A., Fay A. R., Takahashi T., and Metzl, N.: Convergence of atmospheric and
8 North Atlantic carbon dioxide trends on multidecadal timescales. *Nature geoscience*, 4 (9),
9 606-610, 2011.

10 Montegut, C.D., Madec, G., Fischer, A.S., Lazar, A. and Iudicone D.: Mixed layer depth over
11 the global ocean: An examination of profile data and a profile-based climatology. *Journal of*
12 *Geophysical Research-Oceans*. 109, C18, 12003, 2004.

13 Monterey, G. and Levitus, S.: Seasonal variability of mixed layer depth for the World Ocean,
14 NOAA NESDIS Atlas, US Government Printing Office, Washington, DC, 5 pp., 1997.

15 Nightingale, P. D., Malin, G., Law, C. S., Watson, A. J., Liss, P. S., Liddicoat, M. I., Boutin,
16 J., and Upstill-Goddard R. C.: In situ evaluation of air-sea gas exchange parameterizations
17 using novel conservative and volatile tracers, *Global Biogeochem. Cy.*, 14, 373–387,
18 doi:10.1029/1999GB900091, 2000.

19 Padin, X. A., Castro, C. G., Ríos, A. F., and Pérez, F. F.: Oceanic CO₂ uptake and
20 biogeochemical variability during the formation of the Eastern North Atlantic Central water
21 under two contrasting NAO scenarios, *J. Marine. Syst.*, 84, 96–105, 2011.

22 Painter, S. C., Pidcock, R. E., and Allen, J. T.: A mesoscale eddy driving spatial and temporal
23 heterogeneity in the productivity of the euphotic zone of the Northeast Atlantic, *Deep-Sea*
24 *Res. II*, 57, 1281–1292, 2010.

25 Perez, F. F., Mourin C., Fraga, F., and Rios, A. F.: Displacement of water masses and
26 reminer- alization rates off the Iberian Peninsula by nutrient anomalies, *J. Mar. Res.*, 51, 869–
27 892, 1993.

1 Prytherch, J., Yelland, M. J., Pascal, R. W., Moat, B. I., Skjelvan, I., and Neill, C. C.: Direct
2 measurements of the CO₂ flux over the ocean: development of a novel method, *Geophysical*
3 *Research Letters*, 37, doi:10.1029/2009GL041482, 2010.

4 Redfield, A. C.: The biological control of chemical factors in the environment, *American*
5 *scientist*, 64, 205–221, 1958, 1958.

6 Schuster, U. and Watson, A. J.: A variable and decreasing sink for anthropogenic CO₂ in the
7 North Atlantic, *J. Geophys. Res.-Oceans*, 112, C1106, doi:10.1029/2006JC003941, 2007.

8 Schuster, U., Watson, A. J., Bates, N. R., Corbiere, A., Gonzalez-Davila, M. Metzl, N.,
9 Pierrot, D., and Santana-Casiano, M.: Trends in North Atlantic sea-surface fCO₂ from 1990
10 to 2006, *Deep-Sea Res. II*, 56, 620–629, doi:10.1016/j.dsr2.2008.12.011, 2009.

11 Skjelvan, I., Falck, E., Rey, F., and Kringstad, S. B.: Inorganic carbon time series at
12 OceanWeather Station M in the Norwegian Sea, *Biogeosciences*, 5, 549–560,
13 doi:10.5194/bg-5-549-2008, 2008.

14 Takahashi, T., Sutherland, S. C., Wanninkhof, R., Sweeney, C., Feely, R. A., Chipman, D.
15 W., Hales, B., Friederich, G., Chavez, F., Sabine, C., Watson, A., Bakker, D. C. E., Schuster,
16 U., Metzl, N., Yoshikawa-Inoue, H., Ishii, M., Midorikawa, T., Nojiri, Y., Kortzinger, A.,
17 Steinhoff, T., Hoppema, M., Olafsson, J., Arnarson, T. S., Tilbrook, B., Johannessen, T.,
18 Olsen, A., Bellerby, R., Wong, C. S., Delille, B., Bates, N. R. and de Baar H. J. W.
19 Climatological mean and decadal change in surface ocean pCO₂, and net sea-air CO₂ flux
20 over the global oceans, *Deep-Sea Res., Pt II*, 56(8-10), 554-577, doi:
21 10.1016/j.dsr2.2008.12.009, 2009.

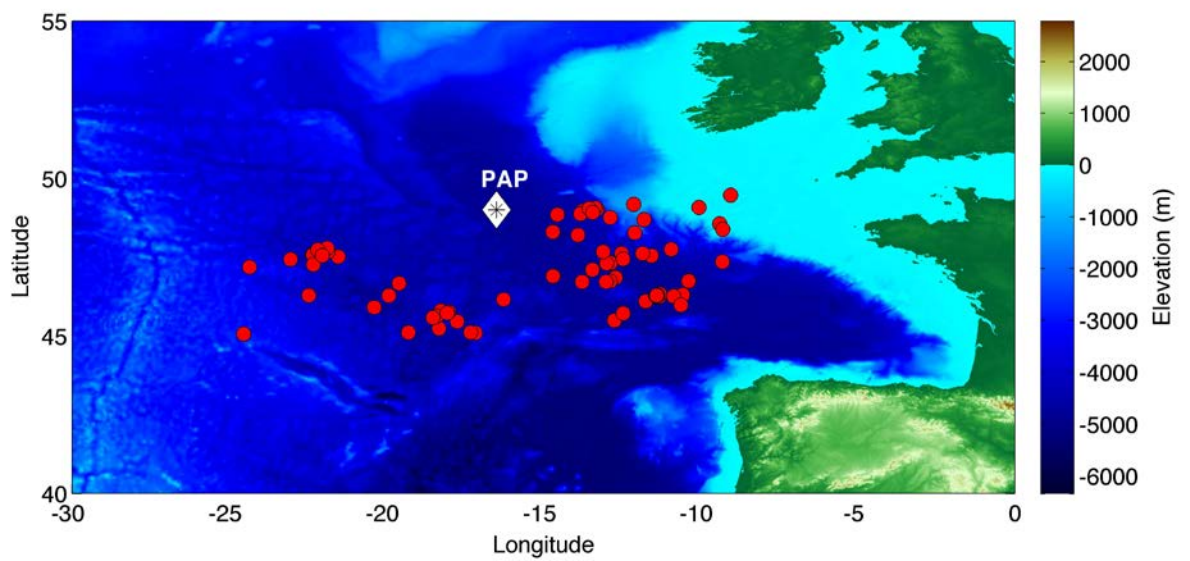
22 Takahashi, T., Sutherland, S. C., Sweeney, C., Poisson, A., Metzl, N., Tilbrook, B., and
23 Bates, N.: Global sea–air CO₂ flux based on climatological surface ocean pCO₂, and
24 seasonal biological and temperature effects, *Deep-Sea Res. II*, 49, 1601–1622, 2002.

25 Thomson, R.E. and Fine, I.V.: Estimating Mixed Layer Depth from Oceanic Profile Data.
26 *Journal of Atmospheric and Oceanic Technology*, 20(2), 319-329, 2003.

27 Wanninkhof, R.: Relationship between wind-speed and gas-exchange over the ocean, *J. Geo-*
28 *phys. Res.*, 97, 7373–7382, doi:10.1029/92JC00188, 1992.

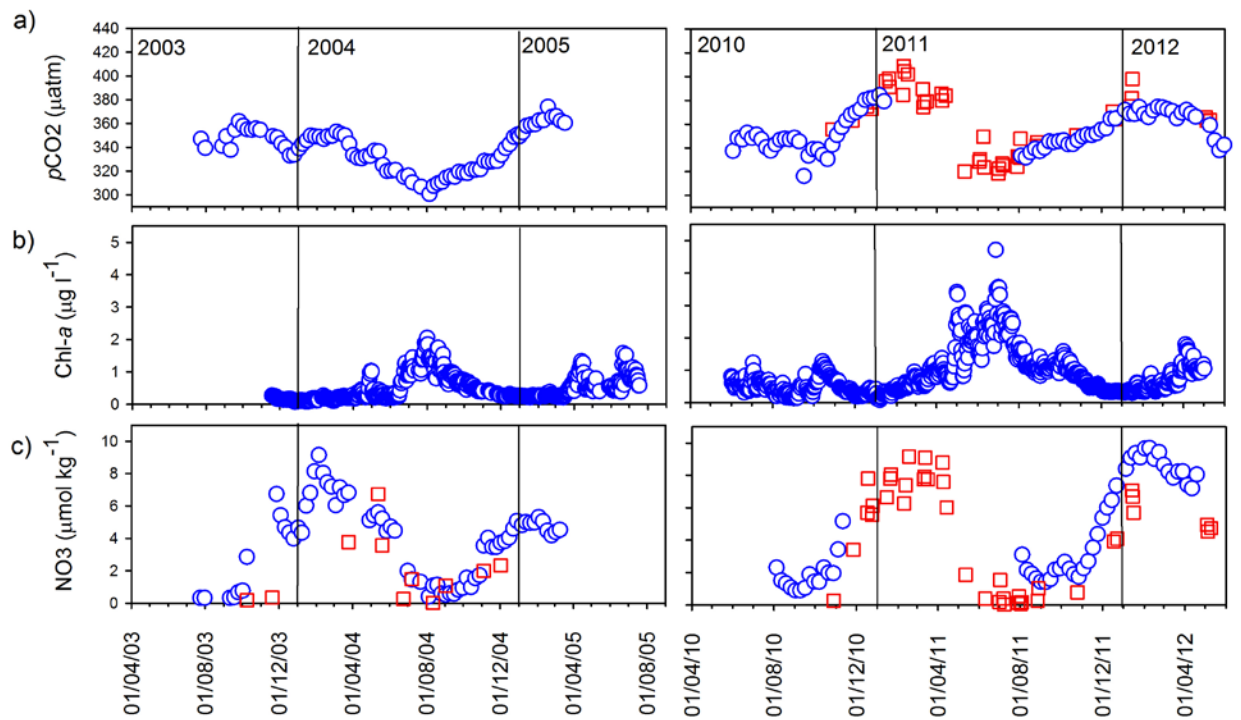
1 Weiss, R. F.: Carbon dioxide in water and seawater: the solubility of a non-ideal gas,
2 Mar.Chem., 2, 203–215, doi:10.1016/0304-4203(74)90015-2, 1974.
3 Williams, R. G., McLaren, A. J., and Follows, M. J.: Estimating the convective supply of
4 nitrate and implied variability in export production over the North Atlantic, Global
5 Biogeochem. Cy., 14, 1299–1313, 2000.

6
7



8
9
10
11

Figure 1. Map of the inter-gyre region of the northeast Atlantic showing the bathymetry around the PAP observatory (white diamond) and the ship of opportunity (SOO) sampling positions (red circles) from 2010 to 2012.



1

2

3 Figure 2. *In situ* 30 m PAP-SO data (blue circles) from 2003–2005 and 2010–2012

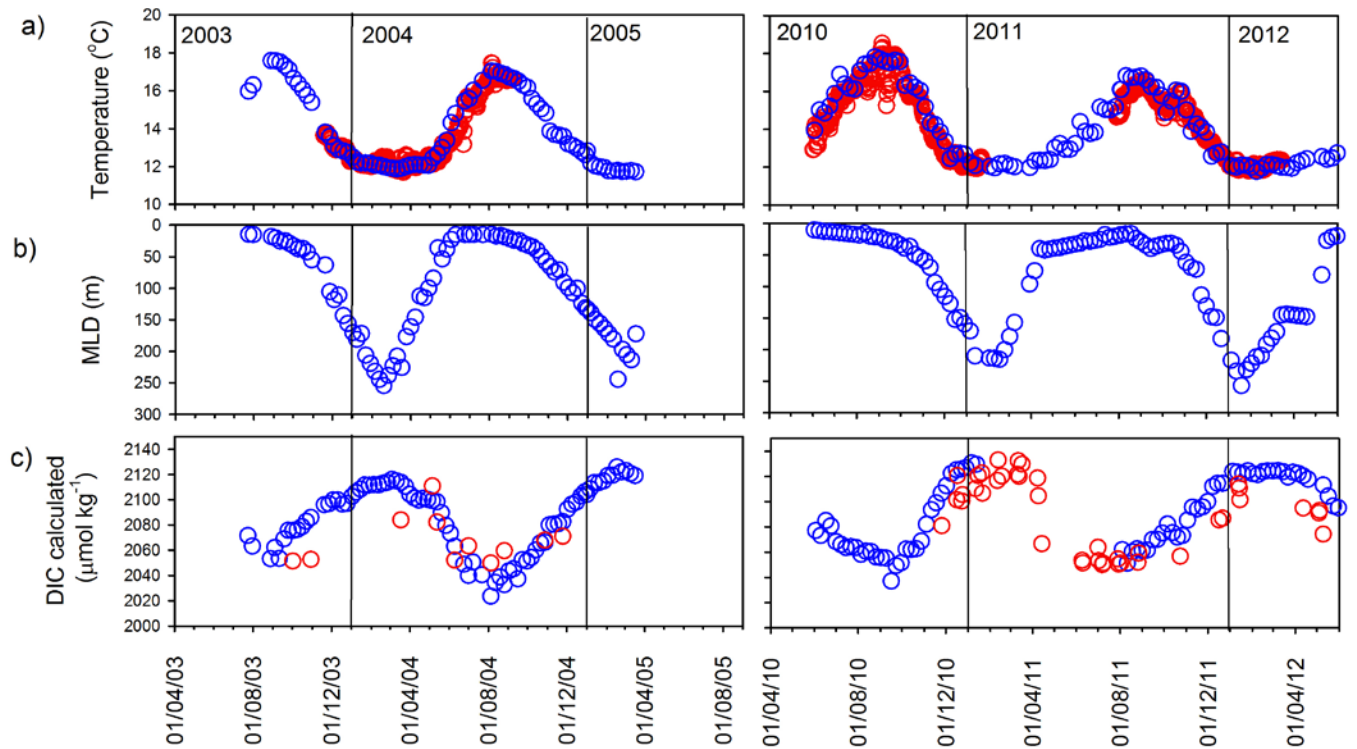
4 and 5 m SOO data (red squares) with vertical lines to represent the start of each year

5 showing: (a) $p(\text{CO}_2)$; (b) chlorophyll a concentration; (c) weekly averaged nitrate

6 concentration.

7

1



2

3

4

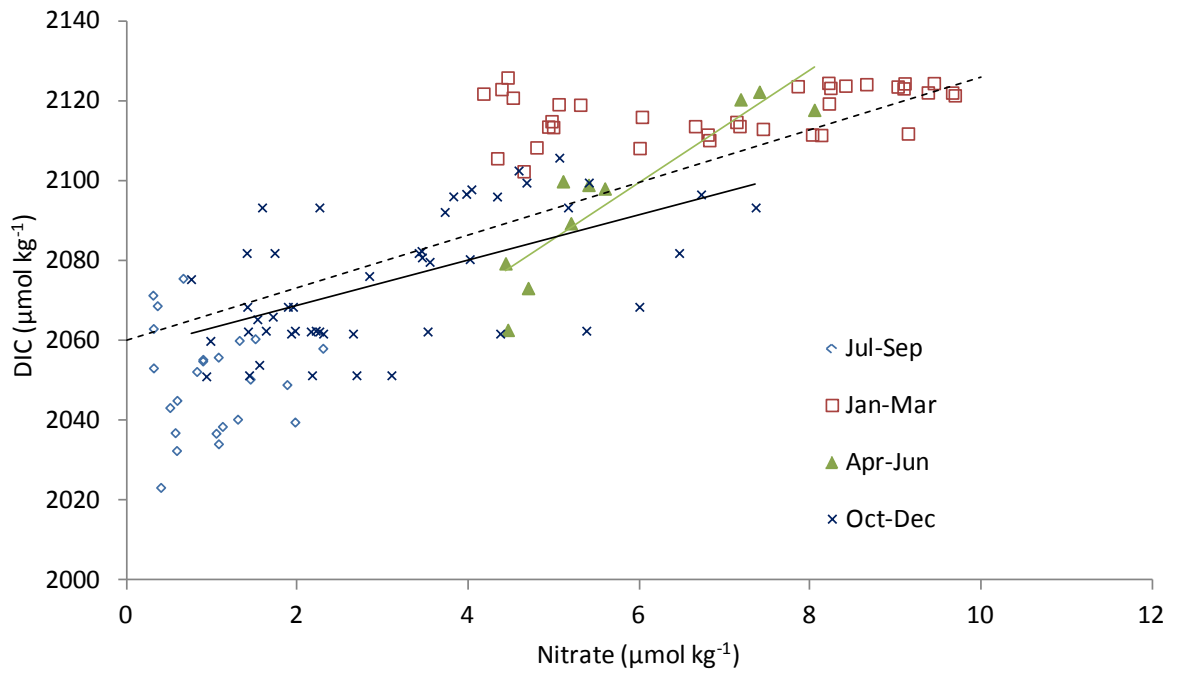
5

6

7

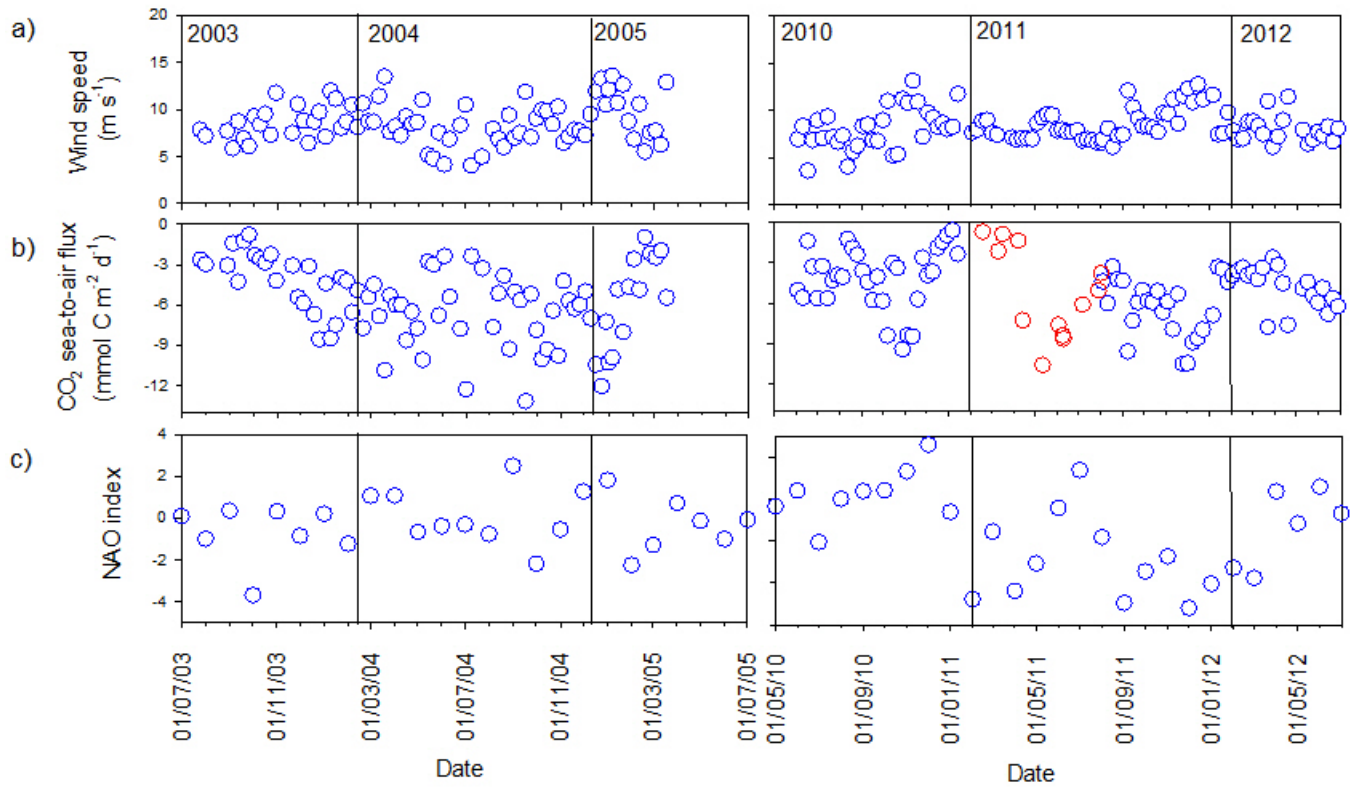
8

Figure 3. Data from 2003–2005 and 2010–2012 (blue circles) with vertical lines to represent the start of each year showing: (a) Argo temperature data from 30 m depth around the PAP-SO and *in situ* MicroCAT temperature data at 30 m (red circles); (b) calculated mixed layer depth (MLD) data; (c) calculations of weekly dissolved inorganic carbon (DIC) concentrations based on *in situ* PAP-SO $p(\text{CO}_2)$ and salinity-based TA parameterisations (see text for details) with additional DIC calculations based on SOO data (red circles).



1

2 Figure 4. The relationship between concentrations of gas exchange-corrected DIC and
 3 nitrate (2010-2012) at the PAP-SO showing 4 different seasons: Winter (January–March, red
 4 squares); Spring (April-June, green triangles); Summer (July-September, blue diamonds);
 5 Autumn (October-December, dark blue crosses). The green line shows the ratio in spring
 6 (14.3) and the blue line is the ratio in autumn (6.4), with the Redfield ratio of 6.6 shown for
 7 reference as a dashed line.



1

2 Figure 5: Data from 2003-2005 and 2010-2012 (blue circles) for (a) weekly satellite wind
 3 data in the region of the PAP-SO; b) calculations of weekly sea-to-air CO₂ flux (negative:
 4 into the ocean) from *in situ* PAP-SO *p*(CO₂) data and satellite wind (see text for details) with
 5 additional flux calculations from SOO data (red circles); c) the monthly NAO index.

6